Czesław Machelski
Prof. dr hab. inż.
Politechnika Wrocławska, Wydział Budownictwa Lądowego i Wodnego;
Katedra Mostów i Kolei
czeslaw.machelski@pwr.edu.pl

DOI: 10.35117/A_ENG_18_10_06

Construction loads of the soil-steel structures

Abstract: A characteristic feature of the soil-steel structure, unlike conventional bridges, is greatly influenced by the backfill ground and the road surface as a load-bearing elements. In the model of soil-steel structure there are two structural parts: steel shell with corrugated pates and backfilling ground with road surface. The interaction between them is modelled as an contact interaction (interface), which is a normal and tangential force to the surface of the shell. The paper provides an algorithm in which the internal forces in the shell are determined on the basis of unit deformations and hence contact effects. The solution uses the condition of compatibility of contact between the soil and the shell and it is allowed to slip at the interface between these two structural parts. In the analysis, attention was paid to the minimum backfilling cover thickness above the shell crown that is safe for construction loads.

Keywords: Soil-steel structures; The backfilling ground impact of the shell; Minimum backfilling cover depth; Construction loads

Introduction

In the thesis, susceptible engineering structures are analyzed on the example of bridge ground and shell structures. Their characteristic feature, unlike the classic bridges, is the high impact of ground backfill and road surface as supporting elements [2],[1]. In the work, the building phase of the object is considered when there is a minimum thickness of the backfilling cover (backfill over the coating) and there is no surface. The results of analyzes - the effects of passing construction vehicles are the effects of ground (backfilling cover) on the structure and internal forces in the shell.

In the initial phase of construction, the load-bearing capacity of the coating in the engineering facility is small. When laying the backfill, the coating is subject to considerable deformation because it is a geometric form limiting the soil in the object being built [2]. Hence, the coating during construction takes over the ground pressure similar to the retaining wall (but susceptible). It is only in the vicinity of backfill that the coating cooperating with the subgrade becomes an effective element of the structure that allows the transfer of significant construction loads, as in Figure 1.

1. Example of constructions load

During the modernization of the surface, as in the final stage of the construction of the object after the level, transport vehicles with large loads and pressure on the wheels pass over the coating. They cause a greater impact on susceptible engineering objects than in the case of the operated object because there is no load distribution through the surface. Important for the safety of the facility is the thickness of the backfill over the coating (backfilling cover).

The dependence of the shell deformation - the impact of the soil

There are two structural subsystems [2],[1],[4],[8] in the models of ground and coating objects: the coating and the remaining part in the form of ground backfill (and the surface with the foundation of the roadway). The interaction between them is modeled as a contact interaction (interface) in the form of surface forces, distributed from the rule into two components: normal p and tangent t, as in Figure 2.

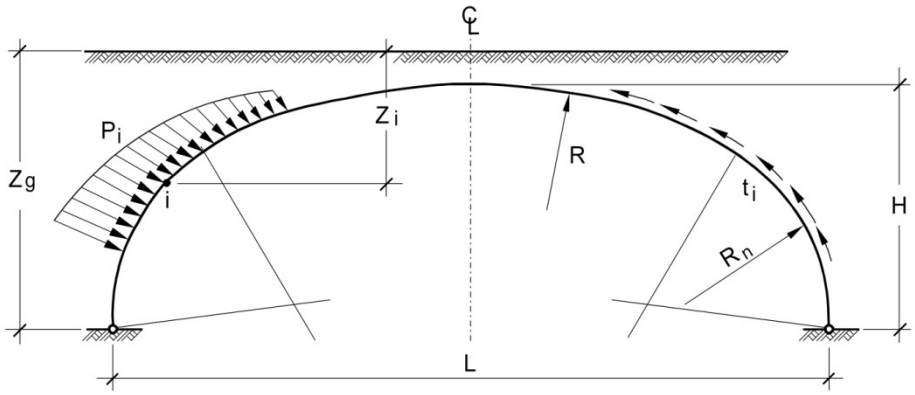

2. Scheme of ground impact forces on the coating in the facility

The work analyzes the upper part of the coating where the radius of curvature is R. This part of the coating undergoes the greatest impacts from commercial vehicles. Effects resulting from the effects of soil on the coating created during the construction and during operation are added together with the effects of moving loads on the bridge. Thus, in the MES model, in which the forces in the soil center are analyzed, it is necessary to map their state from the construction period [2],[8].

In the internal force tests, corrugated coatings use a measuring base made of extensometers. The selected center perimeter band of the object is glued onto electro fume strain gauges accessible from the inside. At each measurement point, the sensors are placed in

pairs, at the top and the crank valley, located in the direction of the perimeter shell band, as in Figure 3.

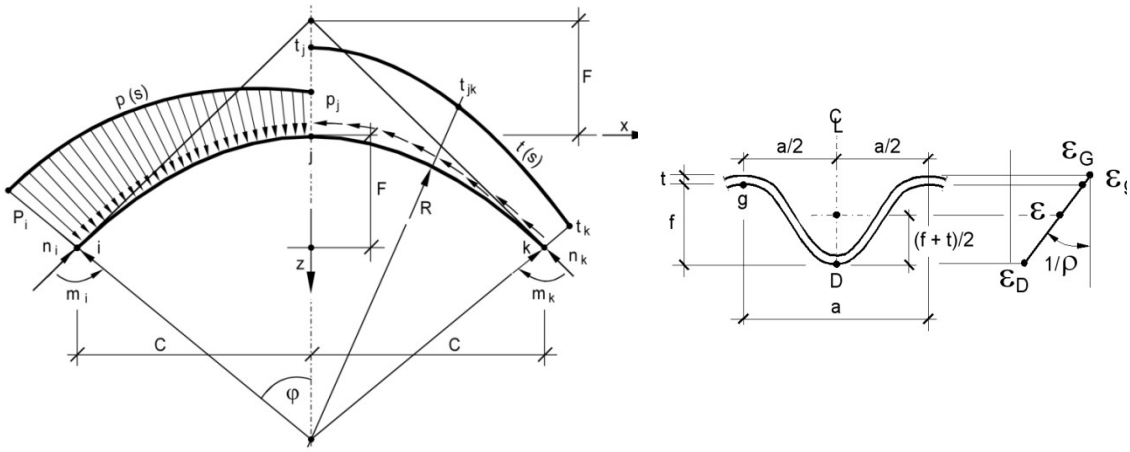

3. Determination of internal forces and contact forces as well as deformations in the shell

The twin sensor system, assuming the principle of flat cross-sections, makes it possible to determine the deformations in the axis of inertia of the corrugated sheet cross-section as in dependence

$$\varepsilon(s) = \frac{\varepsilon_D(f-g) + \varepsilon_g(f+g)}{2f}.$$

(1)

The formula (1) includes the geometry of corrugated sheet, e.g. SC $a \times f \times g$ (wavelength a, its height f and sheet thickness g). To determine the change in the radius of the curvature of the shell ρ, you can use the geometric relationships of the sheet and ε_D and i ε_g as in the equation

$$\kappa(s) = \frac{1}{\rho} = \frac{\varepsilon_g - \varepsilon_D}{f}.$$

(2)

The geometrical quantities determined in formulas (1) and (2) are used to determine the internal forces in the shell: axial force

$$n(s) = \frac{E \cdot A}{a}\varepsilon(s) \tag{3}$$

and bending moment

$$m(s) = \frac{E \cdot I}{a}\kappa(s)$$

(4)

where: A/a= 9,81 mm^2/mm and I/a=24165 mm^4/mm are geometrical characteristics of the cross-section SC 381 × 140 × 7 (wavelength a = 381 mm) while E = 205000 MPa is a feature strength of material (steel).

From the static dependencies of internal forces $n(s)$ and $m(s)$ as a function related to the axis running along the peripheral band of the shell s, we obtain in a differential manner the normal interaction

$$p_j = \frac{m_i - 2m_j + m_k}{b^2} + \frac{n_j}{R}$$

(5)

and tangents

$$t_{jk} = \frac{n_j - n_k}{b} + \frac{m_j - m_k}{b \cdot R}.$$

(6)

The distances between points i, j, k are a circle section, as in figure 3, with the arc length b. The p_j value is calculated at the j -point measurement point, while the t_{jk} force between the j and k points, as in figure 3

Contact impacts

As an example of the research using electro-resistant strain gauges, the results of measurements of the test facility built in Rydzyna [2] were presented, with a record span L = 17,594 m from sheet metal SC 381×140×7, without overlays. The geometrical parameters of the perimeter of the shell in relation to the corrugation's inertia axis are: its height H = 5.459 m and the radius of curvature in the key R = 13.735 m. The thickness of the coat above the coat was h = 1.12 m. The arc lengths between the measurement points are b = 1, 2 m

The position of the vehicle is determined in the drawings relative to the key shell as a co-ordinated x_p. The travel of the loader took place along the perimeter of the shell, in a rolling fashion with Δx_p = 1, 5 m. The pressure on the axles in the loader (without spoil) was similar:

P_1 = 114,3 kN (reference axis) and P_2 = 104,7 kN. The wheelbase (calculated along the shell band) was 3.4 m. The wheel position of the vehicle was symmetrical with respect to the analyzed coating band.

Figures 4 and 5 present changes in the components of contact interactions: normal p and t. Determination of positive p and t values as soil effects per coating is given in Figures 2 and 3. On the horizontal axis of these plots, the value of x_p is given as the distance P_1 from the shell key. In the legend of the drawings, a diagram was drawn up during the primary and return journeys. In both passes the vehicle position is identical, in each setting marked as x_p. The start and end of the measurements was repeated when x_p = 21 m. When x_p = -9 m there was a change in the direction of travel. The specific vehicle positions are:

$x_p < L/4$ = 4,4 m when contact impacts increase;

x_p = 0 when axis P_1 the loader is located above the key;

x_p = - 1,7 m we=hen axes P_1 and P_2 the vehicle are at an equal distance from the key;

x_p = - 3,4 m when axis P_2 is located above the key.

To determine the analyzed points of the shell in Figures 4 and 5, the positions of measurement points were used: x_4 = 1.2 m x_5 = 0 (key) x_6 = -1.2 m. The graphs in Figure 4 are very similar in shape but with significant differences in values during primary and secondary travel. Similar maximum p values in points 4, 5, 6 mean that the area around the shell key is similar to the load on the loader. During the primary run there is no second wave of extreme value when the second axis of the P_2 loader is over the analyzed point. Such extremes are visible at the secondary pass. The conclusion from these analysis results is a significant reduction in the effects of p during the return of the vehicle to the initial state. Thus, there is a hysteresis loop in the case of ground pressure [6],[7].

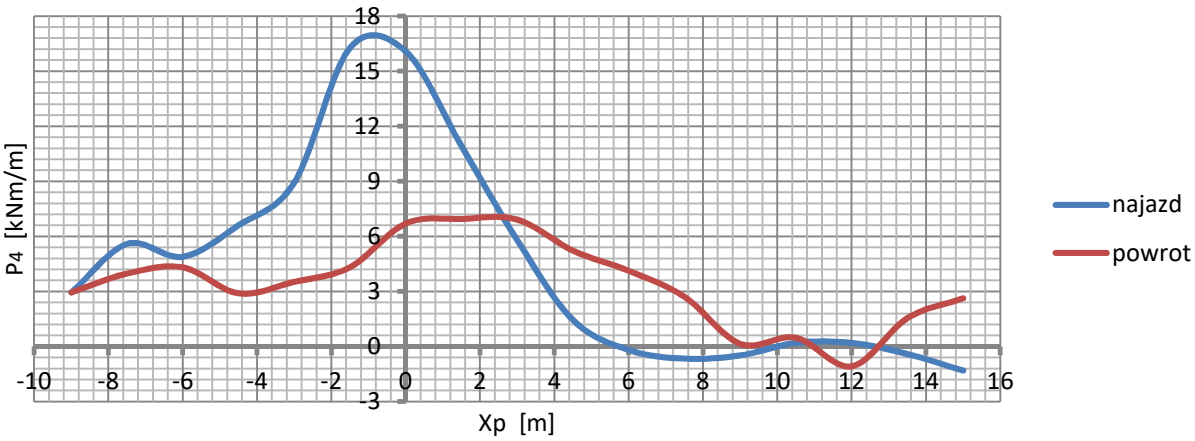

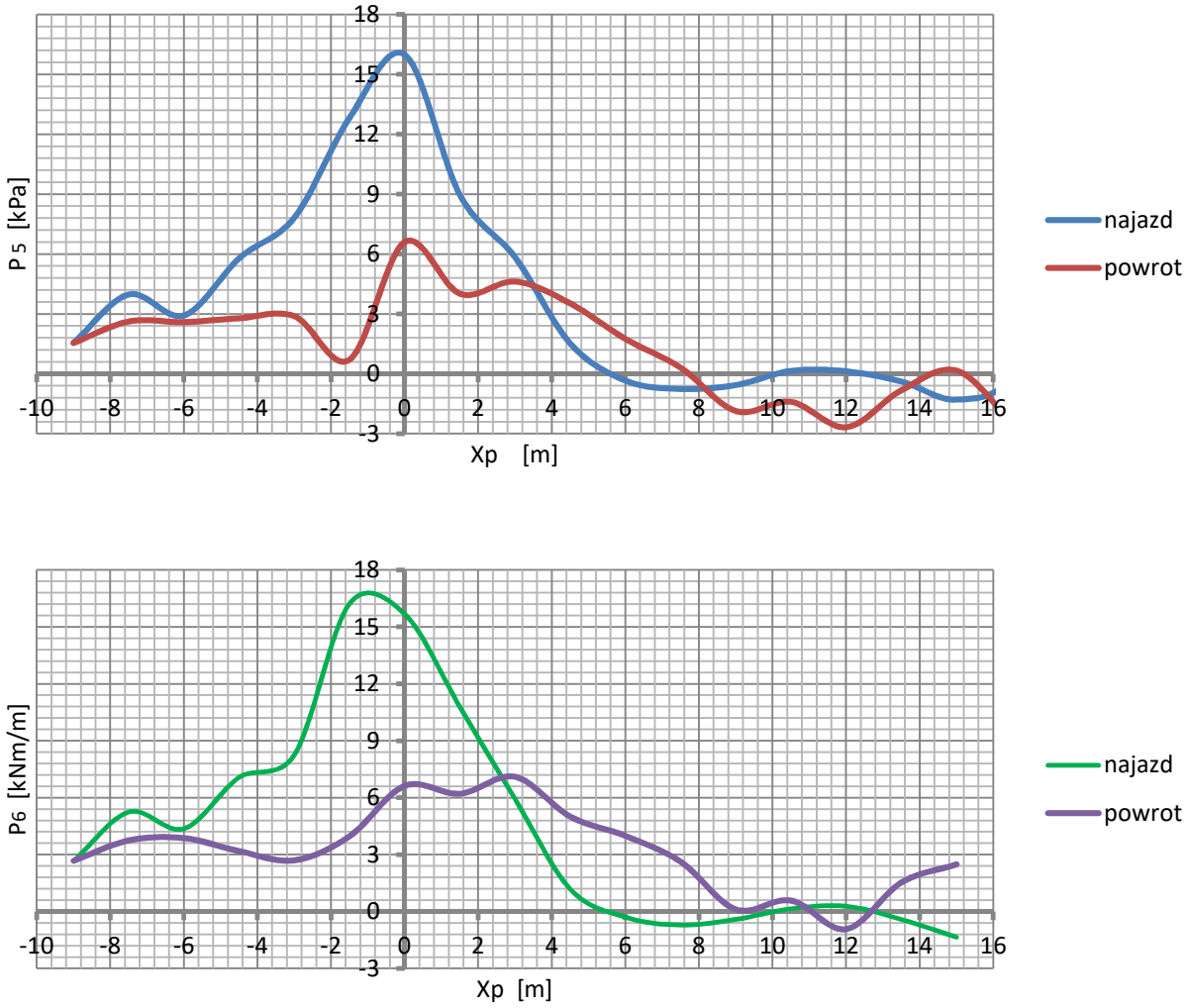

4. Normal interactions in the area of the peripheral band of the shell

Figure 5 presents tangential interaction graphs. Due to the method of their calculation according to formula (6), these are average values between the measuring points on the left and right side of the perimeter band. Tangent forces t_{45} are directed in line (phrases) to t_{56}. Tangent forces t_{46} can be considered values in the shell key only, they are calculated on the basis of distant points 4 and 6 (ie b = 2.4 m) while the two previous graphs are obtained from the shorter range because b = 1.2 m The fundamental difference between the value of t and the pressure is that during the primary and secondary travel functions $t(x_p)$ are similar.

The high t-forces generated during the return of the vehicle to the initial condition are important. The same graphs were also obtained for points located further away from the key but on the opposite side of the shell symmetry axis. Thus, no hysteresis loop is generated in the case of tangential forces. A completely different graph is obtained in the case of tangent forces in the t_{46} shell key. In this case, after the exit of the vehicle, a balanced balance of forces is created, therefore forces t_{45} and t_{56} are similar in value but opposite

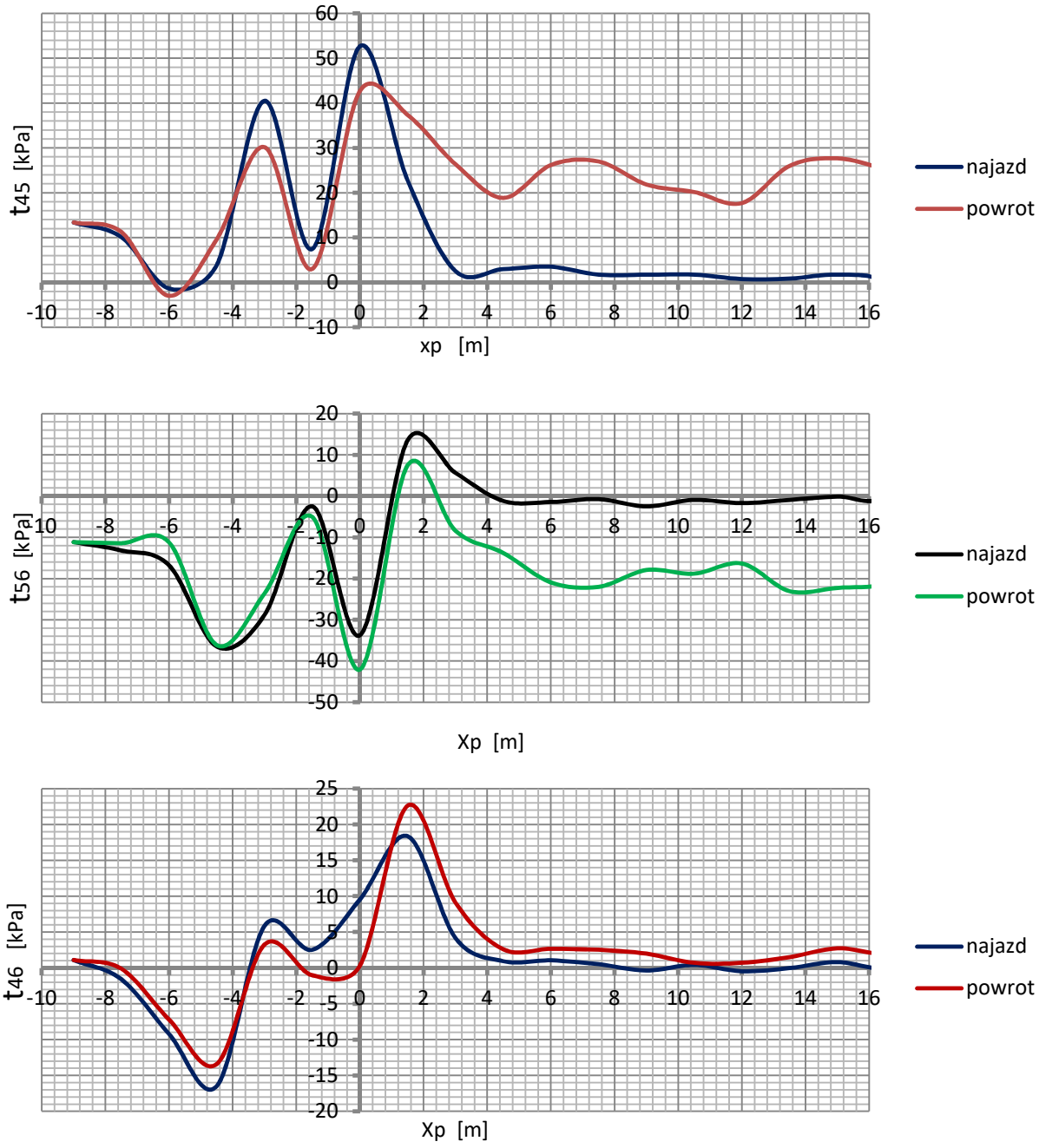

5. Tangent interactions in the area of the peripheral band of the shell

Figure 6 shows the graphs of normal and tangential interactions from one particular vehicle position when $x_p = 0$, i.e. when the force P_1 is above the key of the shell. On the horizontal axis of the graph, the distances of the analyzed points are determined from the shell key s but counted in a radius of radius R. Approaching the shell takes place from the positive side s a return to the opposite side (vehicle settings are identical) and the axis P_2 is above the positive ordinates. From the graph, you can see the position of both axes on the object - very similar during approach and return but with a large difference in value.

In the case of tangent forces, the asymmetrical system of the t(s) graph is visible, which means the inverse return of tangential force in relation to the shell key. These results are confirmed by the graphs t_{46} given in Figure 5. Very large values of t(s) in relation to p(s) are

not an error of the calculation (and measurement) algorithm in this case. In the proposition *t/p* - not exceeding, by definition, the coefficient of friction in the values assigned at work does not take into account the effects of impacts on the weight of groundfill (effects generated during construction). In addition, in the value of t in the corrugated sheet should be reduced by π/2 due to the actual surface impact of tangential forces

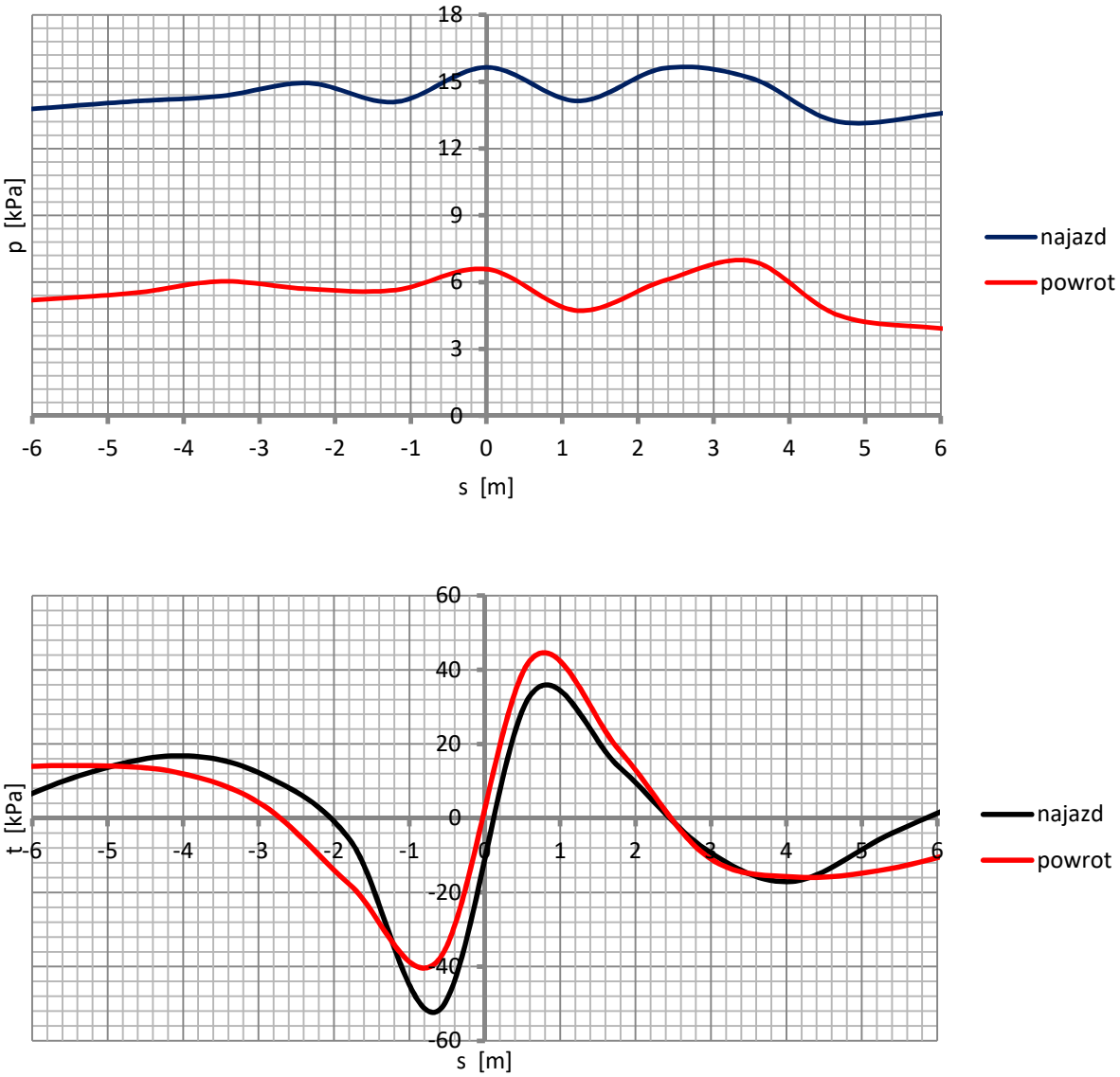

6. Changes in soil pressure in the perimeter of the coating in the load position xp = 0

In the analyzed example of the object, the maximum stress in the corrugated sheet reached a value

$$\sigma = E \cdot \varepsilon = 205000 \cdot 184 \cdot 10^{-6} = 37{,}7 \ \ MPa \, .$$

Cooperation of the backfilling cover with the coating

As an example of the research on the effectiveness of cooperation with the coating with the use of building loads, the results of measurements of the test facility built in Sweden were presented in the paper [5]. The results of the analyzes served to develop guidelines for the design of soil-coating constructions made of corrugated sheets. A closed-shaped coating was

used in the building, as shown in Figure 7, from a sheet with a low profile of MP 200 × 55 × 2.93. The geometric parameters of the peripheral band of the shell related to the corrugation's inertia axis are: the span L = 6,0 m its height H = 4,55 m and the radius of curvature at the key R = 3,052 m. The variable parameter in these tests was the thickness of the above-mentioned coating with set values in table 1.

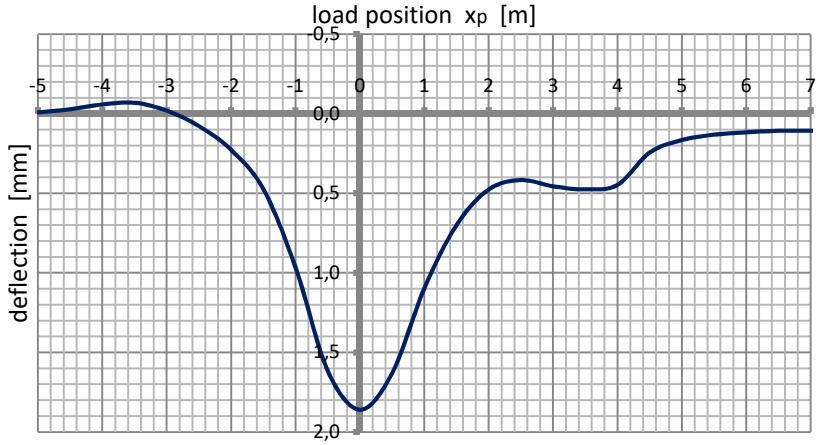

7. Changes in the deflection of the shell key during the travel of the loader [5]

Tab. 1. Maximum values of deflection and internal forces in the shell key as a function of the thickness of the backfilling cover

Analyzed size	Backfilling cover thickness h [m]			
	0,75	0,90	1,20	1,50
w [mm]	6,77	4,22	2,97	1,86
n [kN/m]	121,4	80,4	57,0	43,0
m [kNm/m]	6,93	3,70	1,85	1,10
σ [MPa]	187,8	104,0	56,81	36,36

The tests carried out the transfer of the loader after the object without surface, which is to correspond to the construction situation. The vehicle travel as shown in Figure 7 took place along the perimeter of the shell, in a rolling fashion with Δx_p = 0,5 m. The position of the vehicle was determined in the drawings relative to the key shell as a co-ordinated Δx_p = 0,5 m. The loads on the axles in the loader (with the spoiler) varied: P_1 = 221 kN (reference axis) and P_2 = 69 kN. The wheelbase (calculated along the shell band) was 3.4 m. The displacement sensors and electrofusion strain gauges were the measuring base.

Fig. 7 shows the course of deflection of the shell key in the course of passing the loader when the thickness of the level was h = 1.5 m. The graph shows the effect of the difference of axle loads. When $x_p = 0$, the P_1 force was above the shell key and the maximum deflection occurred. When $x_p = 3.4$ m, the effect of force P_2 appears and the deflection is proportional to the forces smaller. Table 1 presents the maximum values of deflections w and internal forces in the shell key obtained from measurements. The analysis of these quantities as a function of the thickness of the name results in a reduction in the value of building loads. When h <0.75 m, the normal stresses in the coating increase very quickly. Based on the data in Table 1, you can create a stress relationship.

$$\sigma(h) = \left(\frac{17}{4 \cdot h} \right)^3 MPa,$$

(7)

Thus when h = 0.5 m is obtained from (7) σ = 614 MPa. Therefore, with small thicknesses of the hinge, construction loads pose the danger of causing permanent deformation of the coating. In the case of constructed facilities - with the surface there is a significant reduction of deflections and internal forces [2],[3]

Summary

In the work, the construction situation is considered when there is a minimum thickness of the subgrade (overfill over the coating) and there is no surface. This applies to the situation of modernizing the surface of the long-used facility as well as the final construction phase. In this situation, during transport of vehicles with large loads and pressure on wheels, there is a greater impact on susceptible engineering structures than in the operated facility. The paper presents the results of analyzes of soil impact on the structure and displacement and internal forces in the shell as the effects of passing a construction vehicle - a loader. The example indicates the minimum thickness necessary for the passage of heavy construction vehicles. Too small thicknesses may be the reason for the permanent (polastic) deformation of the coating.

The work discusses in detail the algorithm for determining soil contact interactions to the coating in the form of normal tangential components. In the solution, the condition of compliance of contact interactions between soil and coating is used. The principle of compatibility of displacements is not taken into account, i.e. slip in the interface between these sub-systems is allowed. This is an important advantage of the algorithm. The determination of the functions p (s) and t (s) enables a separate analysis of the shell as a separate sub-system - a susceptible engineering object. In soil and shell structures, the impact of moving loads (changing the location) is a separate issue [7],[3],[9].

Source materials

[1] Machelski C, Janusz L.: Application of Results of Test in Developing 2D Model for Soil-Steel Railway Bridges. Journal of the Transportation Research Board. Solid Mechanic, 1/2017 pp. 70-75.

[2] *Machelski C.*: Budowa konstrukcji gruntowo-powłokowych. Dolnośląskie Wydawnictwo Edukacyjne, Wrocław 2013.

[3] *Machelski C.*: Dependence of deformation of soil-shell structure on the direction of load passage. Bridge and Road 13 (2014), pp. 223-233.

[4] *Machelski C.*: Szacowanie oddziaływania zasypki na powłokę w obiekcie gruntowo-powłokowym na podstawie deformacji powłoki . Przegląd Komunikacyjny 11/2016

[5] *Pettersson L.*: Full Scale Tests and Structural Evaluation of Soil Steel Flexible Culverts with low High of Cover. Doctoral Thesis in Civil and Architectural

Engineering Stockholm, 2007.
[6] *Sielver M L, Seed H B*.: Changes in Sands during Cyclic Loading. ASCE Soil Mechanics and Foundations Division Vol. 97, No SM9, September 1971.
[7] *Sobótka M*.: Numerical simulation of hysteretic live load effect in soil-steel bridge. Studia Geotechnika et Mechanica. 36.1 (2014) pp. 103-109.
[8] *Szajna W.S*. Numerical moel for the analysis of construction process of soil-steel culverts. Archives of Institute of Civil Engineering. No 1/2007 p. 215-223.
[9] *White K, Sargand S, Massada T*.: Evaluation of load rating procedure for metal culverts under shallow soil covers. *Archives of Institute of Civil Engineering* 23/2017 pp. 311-323.